AFRL-AFOSR-VA-TR-2024-0116

Energy-efficient Sub-5-nm Magnetic Tunneling Junctions

Osama Mohammed
FLORIDA INTERNATIONAL UNIVERSITY
11200 SW 8TH ST
MIAMI, FL, 33199
USA

01/22/2024
Final Technical Report

Air Force Research Laboratory
Air Force Office of Scientific Research
Arlington, Virginia 22203
Air Force Materiel Command

REPORT DOCUMENTATION PAGE

PLEASE DO NOT RETURN YOUR FORM TO THE ABOVE ORGANIZATION.

1. REPORT DATE	2. REPORT TYPE	3. DATES COVERED	
20240122	Final	START DATE 20181001	END DATE 20210930

4. TITLE AND SUBTITLE
Energy-efficient Sub-5-nm Magnetic Tunneling Junctions

5a. CONTRACT NUMBER	5b. GRANT NUMBER	5c. PROGRAM ELEMENT NUMBER
	FA9550-18-1-0527	61102F

5d. PROJECT NUMBER	5e. TASK NUMBER	5f. WORK UNIT NUMBER

6. AUTHOR(S)
Osama Mohammed

7. PERFORMING ORGANIZATION NAME(S) AND ADDRESS(ES)
FLORIDA INTERNATIONAL UNIVERSITY
11200 SW 8TH ST
MIAMI, FL 33199
USA

8. PERFORMING ORGANIZATION REPORT NUMBER

9. SPONSORING/MONITORING AGENCY NAME(S) AND ADDRESS(ES)	10. SPONSOR/MONITOR'S ACRONYM(S)	11. SPONSOR/MONITOR'S REPORT NUMBER(S)
Air Force Office of Scientific Research 875 N. Randolph St. Room 3112 Arlington, VA 22203	AFRL/AFOSR RTB1	AFRL-AFOSR-VA-TR-2024-0116

12. DISTRIBUTION/AVAILABILITY STATEMENT
A Distribution Unlimited: PB Public Release

13. SUPPLEMENTARY NOTES

14. ABSTRACT
Spintronic/nanomagnetic nanotechnologies are widely considered as a promising alternative tothe semiconductor microprocessor and memory technologies, which are currently facing fundamental limitations in scaling and power consumption. Such devices have advantages of non-volatility in both logic and memory, ultra-low power consumption, radiation hardness, and capability for 3D integration with significantly improved thermal management. However, despite all these advantages, many promising theoretical predictions for these devices have never been realized because of the difficulty to build and test such small devices. For the same reason, the physics in this size has not been fully understood and exploited. In the sub-5-nm size range, device properties become driven by laws of quantum mechanics. The spin excitation's lifespan significantly increases, which in turn due to the rnanoesulting dramatically increased spin accumulation and other quantum-mechanical effects, could lead to
anomalous magnetotransport effects even at room temperature. Understanding the underlying physics in this size range is crucial for discovering and building next-generation spintronic devices. Therefore, the main goal of this project is to use non-traditional nanofabrication
approaches to study the new physics and build such small devices which could effectively leverage the advantageous spintronic properties.

15. SUBJECT TERMS

16. SECURITY CLASSIFICATION OF:			17. LIMITATION OF ABSTRACT	18. NUMBER OF PAGES
a. REPORT	b. ABSTRACT	c. THIS PAGE		
U	U	U	UU	27

19a. NAME OF RESPONSIBLE PERSON	19b. PHONE NUMBER *(Include area code)*
JIWEI LU	00000000

Standard Form 298 (Rev.5/2020)
Prescribed by ANSI Std. Z39.18

Final Progress Report (2018-2021)

Air Force Office of Scientific Research (AFOSR)
Title: "Energy-efficient Sub-5-nm Magnetic Tunneling Junctions"
AFOSR award #: FA9550-18-1-0527
AFOSR Program Officer: Jiwei Lu
PI: Osama Mohammed (original PI: Sakhrat Khizroev, currently with the University of Miami, skhizroev@miami.edu; Ph. 305-284-4789), Florida International University
Date: November 11, 2021

Summary of 3-Year Research Activities

Researchers:
(1). Torres, Ingrid: Ph.D. Graduate Student (Hispanic American, Female) (Graduated with a PhD in 2021)
(2). Navarrete, Brayan: Ph.D. Graduate Student (Hispanic American) (Graduated with a PhD in 2021) (employed as a Senior Engineer at Seagate, Minneapolis, MN)
(3). Dennis Toledo, Graduate Student (Hispanic American) (to graduate in Spring 2023)
(4). Wang, Ping: Ph.D. Graduate Student (Graduated with a PhD in 2020)
(5). Dean, Nathaniel: Undergraduate Student (continued to a PhD program in Physics at UC-Irvine)
(6). Smith, Isadora Takako: Undergraduate Student (Female) (continued as a graduate student at UC-Berkeley)
(7). Stimphil, Emmanuel: Post-doctoral Researcher (African American)
(8). Nagesetti, Abhignyan: Post-doctoral Researcher

Main Accomplishments:

- Development of novel synthesis techniques for ferrimagnetic nanoparticles ranging in size from below 3 to over 10 nm and coreshell magnetoelectric nanostructures (MENs) ranging in size from below 10 to over 20 nm in diameter. To the best of our knowledge, this study has for the first time demonstrated TEM images of coreshell MENs with lattice matched magnetostrictive core and piezoelectric shell (Year 1)
- New physics has been discovered regarding the effect of magnetoelectric coupling between ferromagnetic and ferroelectric materials on the magnetic anisotropy of the magnetic component. Particularly, it was found that the L-S-caused anisotropy effectively increases as a result of this interaction. Such a discovery is an important milestone, particularly for next-generation spintronic based in-memory computing applications (Year 1)
- Building a multijunction nanostructure capable of more than 3 distinct magnetic signals, as confirmed through magneto-optical Kerr effect (MOKE) (Year 1)
- Magnetotransport measuruments of 3- and 4-layer devices (through GMR/TMR studies) have been conducted in collaboration with UC Berkely team (Year 2).
- Build the first STT-based 8-level neuromorphic computing device (Year 3)
- Using Magnetoelectric Nanoparticles (MENPs) As 3D Building Blocks in Next-generation Nanoscale Devices (Year 3)

Outreach Accomplishments:

- Three Hispanic American PhD Graduate Students Including One Woman from underrepresented groups have participated in this research.

- Three PhD Graduate Students including two Hispanic Americans (including one woman) have graduated with their PhD in Electrical and Computer Engineering.
- Two Female Students (One Graduate Student and One Undergraduate Student) have been involved in this research (see above).
- Two Undergraduate Students (Including One Woman) have participated in this research, they continued their studies in graduate schools at UC-Irvine and UC-Berkeley, respectively.

Peer-reviewed Publications where the current AFOSR grant was acknowledged:

1. D. Toledo, B. Navarrete, M. Stone, K. Luongo, P. Wang, P. Liang, and S. Khizroev, "A theoretical study of switching energy efficiency in sub-10-nm spintronic devices," J. Magnetism and Magnetic Materials, accepted on August 30, 2019, Article #: 165776
2. J. Hong, X. Li, O. Lee, W. Tian, S. Khizroev, J. Bokor, L. You, "Demonstration of spin transfer torque (STT) magnetic recording," *Applied Physics Letters* **114**: 243101 (2019)
3. J. Hong, Q. Luo, S. Jung, S. Je, Y. Kim, M. Im, C. Hwang, S. Khizroev, S . Chung, L. You, "Shape transformation and self-alignment of Fe based nanoparticles," Nanoscale Advances, 2019, DOI: 10.1039/C9NA00146H
4. B. Navarrete, M. Stone, , K. Luongo, A. Hadjikhani, P. Wang, J. Hong, P. Liang, J. Bokor, S. Khizroev, "Nanomagnetic particle-based information processing," *IEEE Transactions on Nanotechnology (IEEE T-Nano)*, DOI: 10.1109/TNANO.2019.2939009.
5. J. Hong, M. Stone, B. Navarrete, K. Luongo, J. Bokor, S. Khizroev, "Multilevel three-dimensional spin computer," *Applied Physics Letters* **112**, 112402-4 (2018)
6. P. Wang, E. Zhang, D. Toledo, I.T. Smith, B. Navarrete, N. Furman, A.F. Hernandez, M. Telusma, D. McDaniel, P. Liang, and S. Khizroev, "Colossal magnetoelectric effect in coreshell magnetoelectric nanoparticles," *Nano Letters*, doi.org/10.1021/acs.nanolett.0c01588, 2020
7. S. Khizroev and P. Liang, "Engineering future medicines with magnetoelectric nanoparticles: wirelessly controlled, targeted therapies," *IEEE Nanotechnology Magazine* **14** (1): 23-29; 10.1109/MNANO.2019.2952227
8. P. Wang, D. Toledo, E. Zhang, M. Telusma, D. McDaniel, P. Liang, S. Khizroev, "Scanning probe microcopy study of cobalt ferrite-barrium titanate coreshell magnetoelectric nanoparticles," accepted with minor revisions to Journal of Magnetism and Magnetic Materials (JMMM), 2020
9. J. Hong, X. Li, N. Xu, H. Chen, S. Cabrini, S. Khizroev, J. Bokor, L. You, "A dual magnetic tunnel junction-based neuromorphic device," *Advanced Intelligent Systems*: 2000143 (2020)
10. R. Guduru, P. Liang, A. Hadjikhani, P. Wang, V. Musaramthota, A. Franco Hernandez, B. Arkook, J. Hong, S. Khizroev, "Magnetically controlled crystallographic properties of graphite sheets with self-assembled periodic arrays of magnetoelectric nanoparticles," *Appl. Surf. Science* **573**: 151455 (2021).
11. P. Wang, D. Toledo, E. Zhang, M. Telusma, D. McDaniel, P. Liang, **S. Khizroev**, "Scanning probe microcopy study of cobalt ferrite-barium titanate coreshell magnetoelectric nanoparticles," JMMM 516: 167329 (2020).
12. M. Pardo, E. Roberts, K. Pimentel, Y. Yildirim, B. Navarrete, P. Wang, E. Zhang, P. Liang, **S. Khizroev**, "Size-dependent intranasal administration of magnetoelectric nanoparticles for targeted brain localization," *Nanomedicine: NBM* **32**: 102337 (2021).

Year 1 Progress Report (2018-2019)

Summary

Researchers:
Several researchers have been recruited at Florida International University (FIU) to work on this project. Besides the above PI, they include:
(1). Torres, Ingrid: Ph.D. Graduate Student (Hispanic American, Female)
(2). Navarrete, Brayan: Ph.D. Graduate Student (Hispanic American)
(3). Dennis Toledo, Graduate Student (Hispanic American)
(4). Wang, Ping: Ph.D. Graduate Student
(5). Dean, Nathaniel: Undergraduate Student
(6). Smith, Isadora Takako: Undergraduate Student (Female)
(7). Stimphil, Emmanuel: Post-doctoral Researcher (African American)
(8). Nagesetti, Abhignyan: Post-doctoral Researcher

Main Accomplishments:

- Development of novel synthesis techniques for ferrimagnetic nanoparticles ranging in size from below 3 to over 10 nm and coreshell magnetoelectric nanostructures (MENs) ranging in size from below 10 to over 20 nm in diameter. To the best of our knowledge, this study has for the first time demonstrated TEM images of coreshell MENs with lattice matched magnetostrictive core and piezoelectric shell (Fig. 1).
- New physics has been discovered regarding the effect of magnetoelectric coupling between ferromagnetic and ferroelectric materials on the magnetic anisotropy of the magnetic component. Particularly, it was found that the L-S-caused anisotropy effectively increases as a result of this interaction. Such a discovery is an important milestone, particularly for next-generation spintronic based in-memory computing applications (Fig. 2).
- Building a multijunction nanostructure capable of more than 3 distinct magnetic signals, as confirmed through magneto-optical Kerr effect (MOKE) (Fig. 3).
- Design and completion of a test structure to measure magnetotransport characteristics of novel nanodevices (a paper is accepted to a peer-reviewed journal, IEEE Transactions of Nanotechnology (T-Nano) [3])

Outreach Accomplishments:

- Four Graduate Students from underrepresented groups have been involved in this effort (see above).
- Two Female Students have been involved in this research (see above).
- Two Undergraduate Students have been involved (see above).

Goals for Year 2:

- Magnetotransport measurements of magnetoelectric nanodevice, preferably cryogenic measurements
- Build a device based on the spin-transfer torque (STT) effect to record into the described 3-D magnetic nanostructures. (Alternatively, build a device based on the giant magnetoresistance (GMR) or tunneling magnetoresistance (TMR) to read information back from the described 3-D magnetic nanostructures.)

Peer-reviewed Publications where the current AFOSR grant was acknowledged:

13. D. Toledo, B. Navarrete, M. Stone, K. Luongo, P. Wang, P. Liang, and S. Khizroev, "A theoretical study of switching energy efficiency in sub-10-nm spintronic devices," J. Magnetism and Magnetic Materials, accepted on August 30, 2019, Article #: 165776
14. J. Hong, X. Li, O. Lee, W. Tian, S. Khizroev, J. Bokor, L. You, "Demonstration of spin transfer torque (STT) magnetic recording," *Applied Physics Letters* **114**: 243101 (2019)
15. J. Hong, Q. Luo, S. Jung, S. Je, Y. Kim, M. Im, C. Hwang, S. Khizroev, S . Chung, L. You, "Shape transformation and self-alignment of Fe based nanoparticles," Nanoscale Advances, 2019, DOI: 10.1039/C9NA00146H
16. B. Navarrete, M. Stone, , K. Luongo, A. Hadjikhani, P. Wang, J. Hong, P. Liang, J. Bokor, S. Khizroev, "Nanomagnetic particle-based information processing," *IEEE Transactions on Nanotechnology (IEEE T-Nano)*, DOI: 10.1109/TNANO.2019.2939009.
17. J. Hong, M. Stone, B. Navarrete, K. Luongo, J. Bokor, S. Khizroev, "Multilevel three-dimensional spin computer," *Applied Physics Letters* **112**, 112402-4 (2018)

Detailed Description of Research Activities

(1). Synthesis of different size and composition MENPs

We have synthesized new types of MENPs. With respect to the composition, new MENPs were made also of Ni-ferrite cores, in addition to the standard Co-ferrite cores. With respect to the size, we have changed both, the core size and the shell size, through chemical and thermal synthesis variations. A typical transmission electron microscopy (TEM) image showing a perfect 15-nm Co-ferrite based MENP is shown in Fig. 1a. To the best of our knowledge, it is the smallest coreshell magnetoelectric nanostructure ever produced with clearly observed perfectly matched (at the interface) crystal structures of the magnetostrictive Co-ferrite core and the piezoelectric barium titanite shell. The perfect lattice matching is vital for maximizing the magnetoelectric coupling in these nanostructures. Currently, we are working on preparation of a paper to a high-impact scientific journal. One way to control the ME coefficient in these nanostructures is by changing the core-to-shell ratio in these nanocomposites. For examples, TEM images of MENPS with two different core-to-shell ratio values, with the shell thicker and thinner than the core, respectively, are shown in Figs. 1b left and right, respectively. In all the experiments, the shell is made of the popular barium titanite crystal structure. The size of these nanostructures can be controlled many different ways, e.g., through the size of the core or shell components, through thermal control of all the chemical steps involved in the synthesis. For example, TEM images of three different sizes of the Co-ferrite nanoparticles, 3, 6, and 10 nm, respectively, are shown in the top row of Fig. 1c. TEM images of the MENPs made of these core components by adding the same piezoelectric shell are shown in the bottom row, respectively.

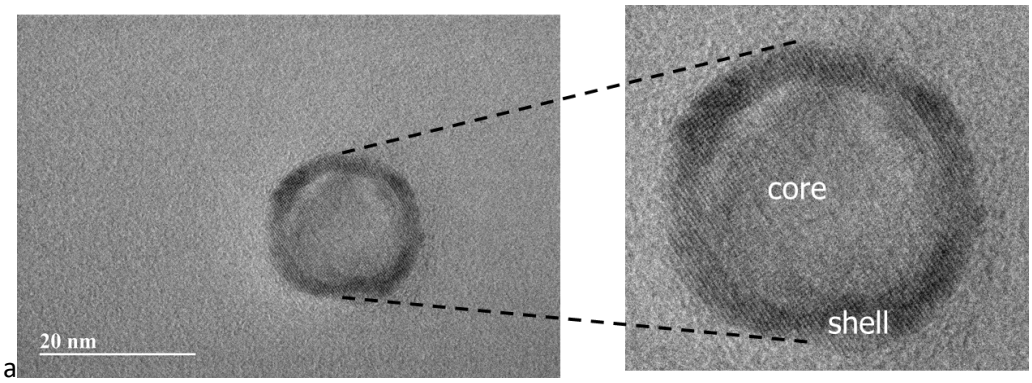

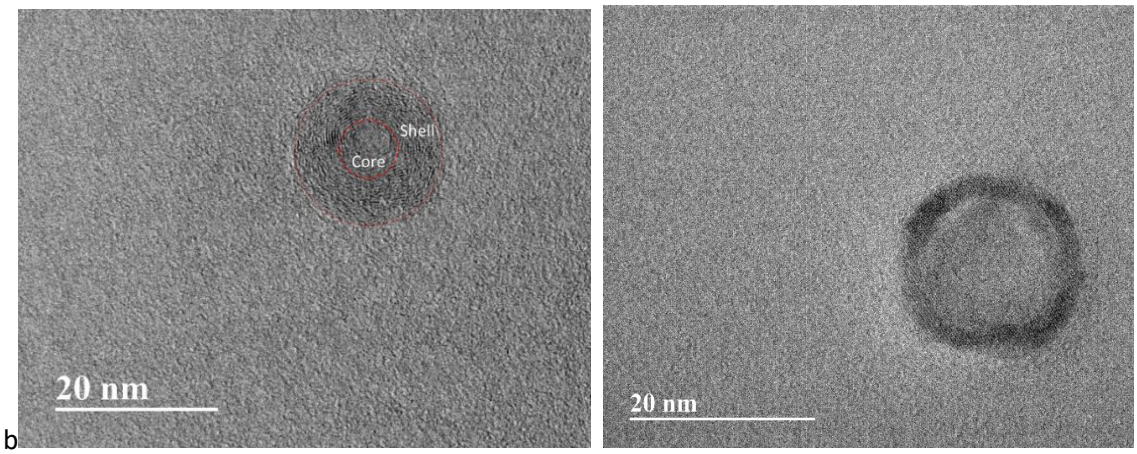

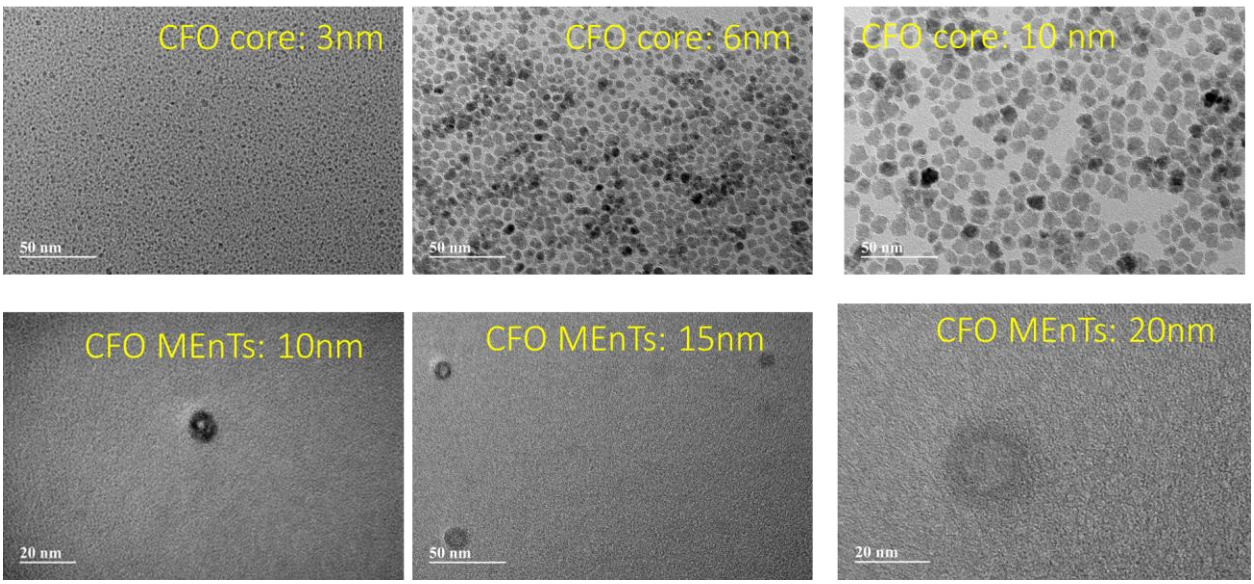

Figure 1: **(a)** TEM image of a 15-nm MENP. The image on the right shows a zoomed-in picture with clearly observed perfectly matched (at the interface) crystal structures of the magnetostrictive $CoFe_2O_4$ core and the piezoelectric $BaTiO_3$ shell. The perfect lattice matching is vital for maximizing the magnetoelectric coupling in these nanostructures. **(b)** TEM images of Co-ferrite based MENPs with two different values of the core-to-shell ratio ratio: (left) 1:2 and (right) 2:1. **(c)** Top Row: Transmission electron microscopy (TEM) images of 3 sizes of Co-ferrite nanoparticles: 3, 6, and 10 nm. Bottom row:

TEM images of 3 sizes of $CoFe_2O_4$-$BaTiO_3$ MENPs made of these cores with lattice matched to the piezoelectric perovskite shells: 10, 15, and 20 nm.

(2). Characterization of new types of MENPs

We have extensively characterized new MENPs. The conducted experiments include vibrating sample magnetometry (VSM) and alternating gradient magnetometry (AGM) studies of M-H loops, X-Ray diffraction (XRD) measurements, atomic force microscopy (AFM), and last but not least direct measurements of the magnetoelectric effect (ME).

(a). Magnetometry measurements: Figs. 2a shows a typical M-H loop measured via VSM of Co-ferrite based MENPs in a powder form. For comparison, Fig. 2b shows a typical M-H curve for a powder made of the core nanoparticles of which these MENPs are made, particularly 10-nm Co ferrite. It can be noted that the saturation magnetization of the core nanoparticles is higher, as expected. Here, it is can be noted that the M-H loops are isotropic because the nanoparticles have been measured in a powder form, without identifying any specific measurement orientation. In the future, we will deposit MENPs on special substrates to make sure their anisotropic "easy" axes are aligned with respect to the substrate and thus allow to measure their magnetic anisotropy, which in turn is affected by the magnetoelectric coupling.

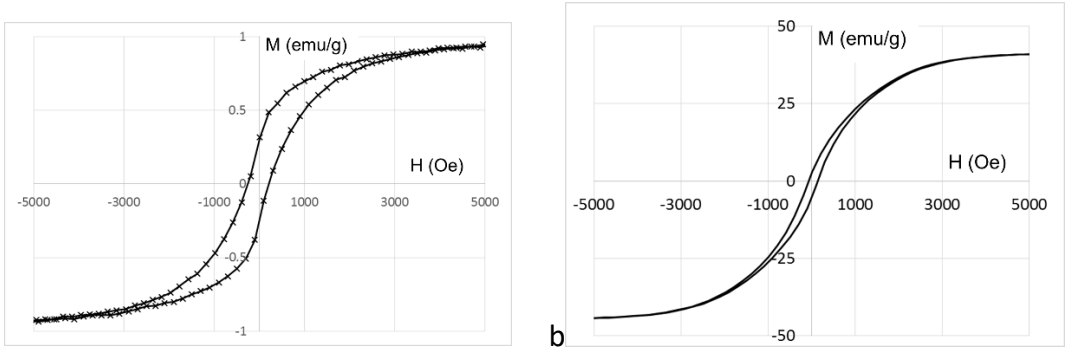

Figure 2: (a) M-H loop (with VSM) of "20-nm MENTs" of the default coreshell composition (powder form). (b) M-H loop of 10-nm Co-ferrite core nanoparticles of which the "20-nm MENTs" are made. The measurements are taken via VSM.

Fig. 3 shows M-H loops of 10-nm Ni-ferrite core nanostructures and MEnTs based on these cores. To conduct these measurements, these nanoparticles were specially deposited on a non-magnetic substrate with a bias magnetic field applied normal to the substrate. Then, M-H loops were measured with two orientations of the applied magnetic field, in plan (IP) and out-of-plane (OOP), respectively. Compared to the M-H loops for the traditional Co-ferrite core nanostructures, these loops show no hysteresis. Therefore, these nanoparticles are in the superparamagnetic phase. Their saturation magnetization, M_s, is on the order of 0.002/6x10^-5 ~ 30 emu/g, which is higher than that for the Co-based counterparts (~10 emu/g). The signal which can be read back from these NPs is proportional to M_s^2 and thus should be an order of

magnitude higher than that from the Co-based MEnTs. Also, the saturation magnetization defines the ability to sense/control these NPs via magnetic detection/control techniques. Interestingly, adding the piezoelectric shell to the core increases the coercivity field (to ~50 Oe), which also indicates an increase of the intrinsic anisotropy field. The latter can be explained by an effective field due to the ME coupling. It is a novel physics, which has never been observed before. We will further explore this phenomenon.

a 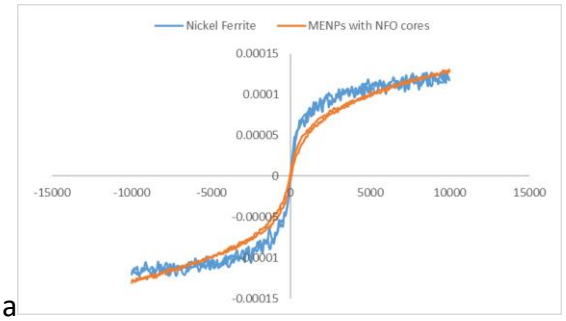

b 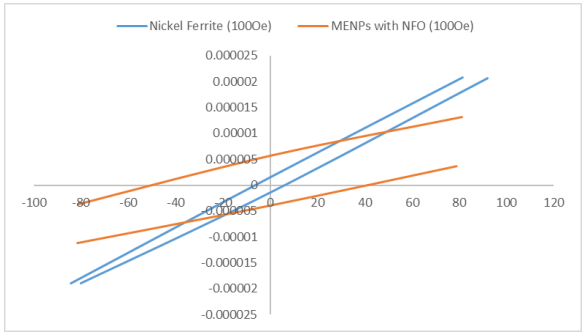

Figure 3: (a) M-H loop (with AGM) of 10-nm Ni-ferrite cores (superparamagnetic) and MENPs based on these cores. (b) Zoomed-in M-H loops to show the coercivity values.

<u>b). Magneotelectric Coefficient Measurements</u> (a novel approach to directly measure the ME coefficient at a single-nanoparticle level):

The magnetoelectric (ME) coefficient is the key property of MENPs. In the past, we had measured the ME coefficient according to the traditional power setting. In this project, we have used a relatively new approach which we recently developed to measure the ME coefficient of individual nanoparticles. It is noteworthy that the traditional powder form cannot represent the correct value of the ME coefficient because of the strong inter-particle contribution to the net effect. In contrast, we have precisely measure the ME coefficient from a few single nanoparticles using a locked-in point contact approach. Furthermore, to confirm the validity of this method, we have implemented two different versions of this new approach. One version is based on the existing scanning tunneling microscopy (STM) mode known as scanning tunneling spectroscopy (STS); we have custom modified the STS setup to include a solenoid coil wrapped around the silicon etched nanoprobe. This version provides the ME coefficient measured from individual nanoparticles in a d.c. approach. In contrast, the other version is an a.c. approach, it is based on a specially made (through 3d printing) nanoprobe, which is brought in contact via sub-micron steps (through a piezo actuator). A photograph of the setup is shown in Fig. 4a. After a contact being established, using a lock-in amplifier, an a.c. voltage is measured across the nanoparticle at the same frequency and phase locked-in to an electric current signal sent to a micro-solenoid wrapped around the nanoprobe. Interestingly, the both versions, d.c. and a.c., respectively, resulted in a similar value of the ME coefficient, on the order of 1 V $cm^{-1}Oe^{-1}$, which is at least one order of magnitude higher than the maximum value reported through the traditional powder techniques. The dependences of the ME coefficient on the a.c. magnetic field strength and frequency for the both Co- and Ni-based MENPs are summarized in Figs. 4b and c, respectively. The Co- and Ni-ferrite MENPs have shown the ME coefficient at zero frequency on the order of 6 and less than 0.1 V cm^{-1} Oe^{-1}, respectively. However, the frequency dependence for the MENPs of

these two materials have been quite different. The ME coefficient of the Co-based MENPs seem to be only weakly dependent on the frequency in the range under study (0-100 Hz). In contrast, the ME coefficient for the Ni-based MENPs strongly depends on the frequency, the coefficient significantly increases to over 1 V cm^{-1} Oe^{-1} by the highest frequency value of 100 Hz. While there is only an insignificant difference between the d.c. and a.c. response for the Co-based nanoparticles, there is a great different between the d.c. and a.c. response for the Ni-based nanoparticles. In fact, for the latter, there is barely any detectable ME coefficient at zero frequency, while the ME values grows quite rapidly with frequency under the studied range. The difference might be due to the superparamagnetic nature of the Ni-based ferrite nanoparticles in this range. For example, one can see that only after the frequency increases above approximately 5 Hz, the ME value becomes significant. We will study this physics in the near future.

a 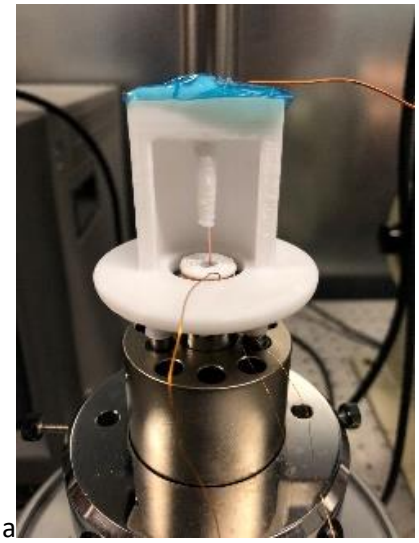

b 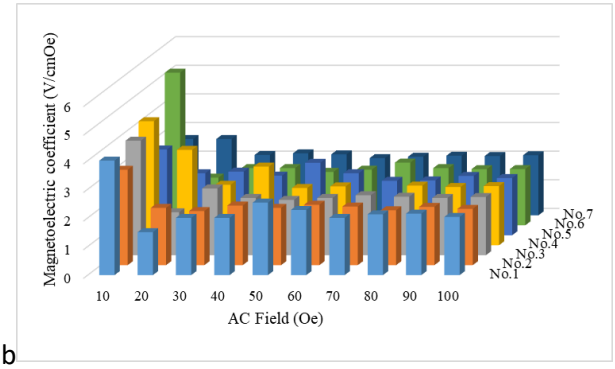

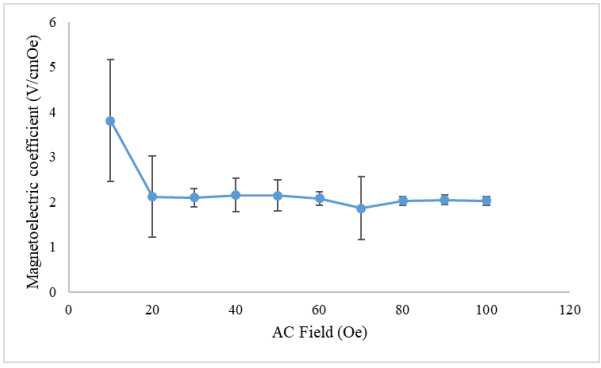

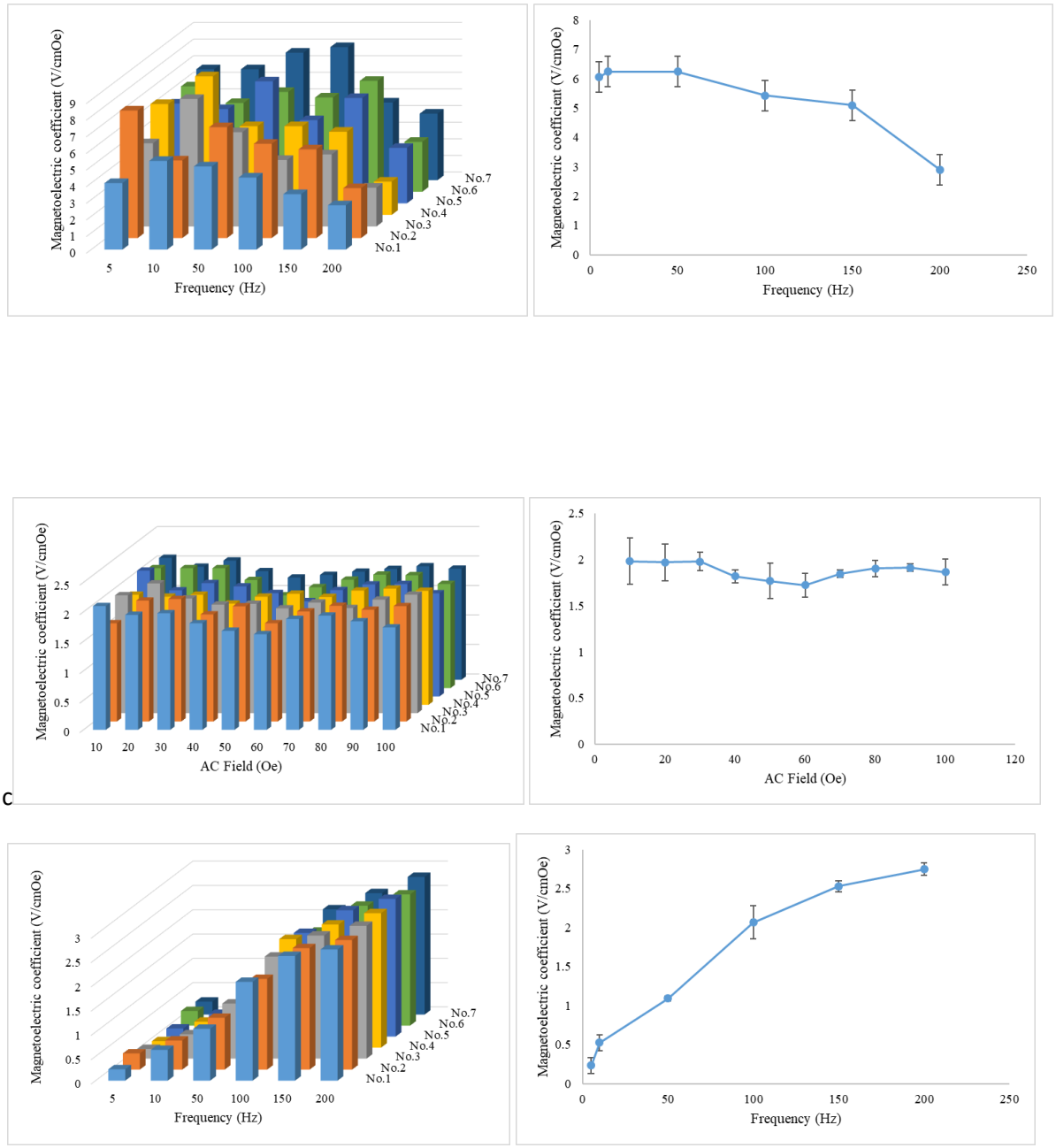

c

Figure 4: (a) Photograph of the a.c. nanoprobe setup for measuring the ME effect. Dependence of the magnetoelectric coefficient on (b) ME coefficient for Ba-ferrite based MENPs: The magnetoelectric (ME) coefficient is shown as a function of the a.c. field strength (at 100 Hz) (top row) and frequency (at 30 Oe) (bottom row). Each dependence is shown as a 3D chart and a 2D plot with an error bar. The error bar for each point is obtained as a result of averaging over 7 measurements. (c) ME coefficient for Ni-ferrite based MENPs: The magnetoelectric (ME) coefficient is shown as a function of the a.c. field strength (at 100 Hz) (top row) and frequency (at 30 Oe) (bottom row). Each dependence is shown as a 3D chart and a 2D plot with an error bar. The error bar for each point is obtained as a result of averaging over 7 measurements.

c) XRD Diffraction Studies: A XRD study of the novel Ni-based MENPs is important to confirm the presence of Co- or Ni- crystallographic orientations in the final coreshell MEnTs. The key property of these NPs, i.e., the non-zero ME coefficient, is a result of a lattice matching between the ferrite core and the barium titanite shell. For example, for the Ni-based MEnPs, we rely on matching between the directions 220 of the core and 110 of the shell, as shown in Fig. 5. One clearly can see the resulting peak in the XRD spectrum. The presence of other slightly shifted peaks is a signature of the lattice matching process characteristic to heterostructured nanocomposies.

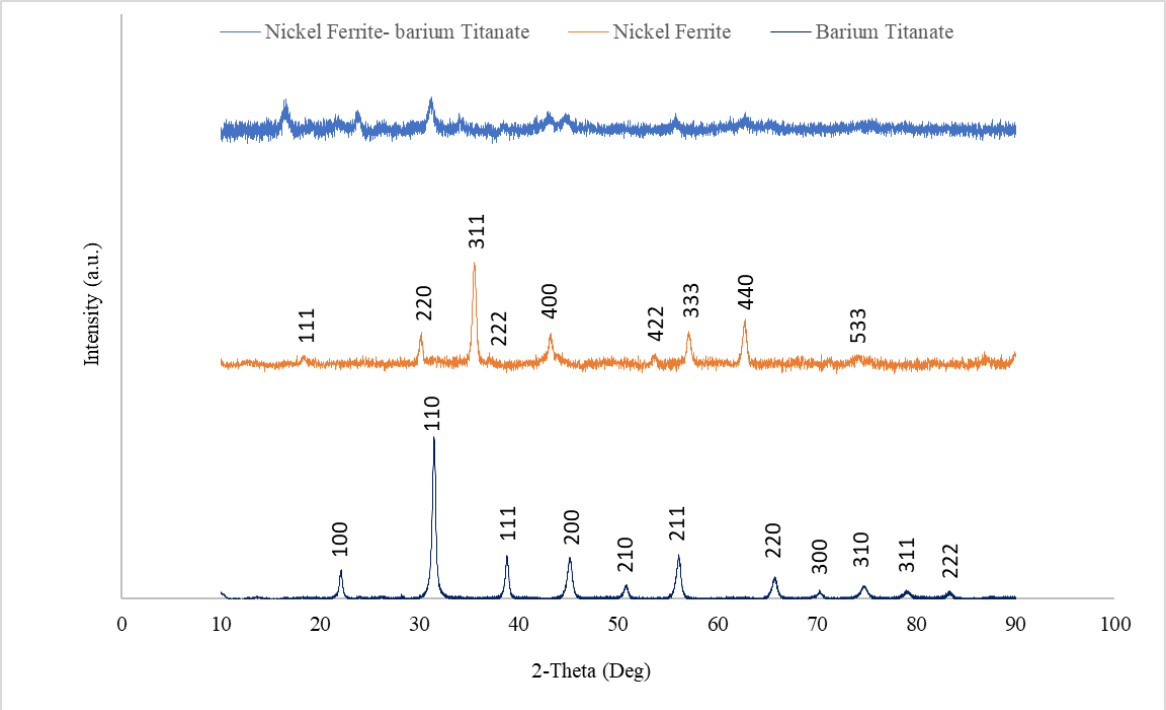

Figure 5: XRD studies of Ni-based ferrite cores, barium titanite shells, and the final 25-nm MENPs made of these core and shell nanostructures.

(3). Multilevel 3-D Magnetic Nanostructures

To create a multilevel device, information has been recorded into a stack of weakly coupled magnetic layers. Each layer is made of a high anisotropy magnetic material, e.g., CoFeB or Co/Pt and/or Co/Pd pairs. Each layer is approximately 0.5 to 2 nm thick. The thickness of the separating layer, e.g., MgO or Pt or Pd, controls the exchange coupling between adjacent layers. While sub-layers (or pairs) in each layers are relatively strongly exchange coupled (via keeping the physical separation on the order of 1 nm and less), all the adjacent layers are relatively weakly exchange coupled (by keeping the respective separation layers 1 to 2 nm thick) so that different layers can be independently recorded. By controlling the coercivity of the magnetic layers across the multilayer stack, it is possible to write and read multilevel signal from the media. A typical focused magneto-optical Kerr effect (f-MOKE) signal measured from a 3-layer stack is shown in Fig. 6a. Clearly, 8 signal levels can be generated in such a structure (with a net thickness of less than 20 nm). An atomic force microscopy (AFM) image of the surface of a typical multilayer-based 3-D media is shown in Fig. 6b. One can clearly a granular surface with a roughness on the order of a nanometer. Our goal is to improve the roughness so that we could

create more than 3 layers. Next year, our focus will be on using spin-transfer torque (STT) effect to write in such a media. We have conducted and published preliminary experiments which have proven the feasibility of this concept [In the list of the published papers, reference #5]. We will try to build a robust device based on the novel concept.

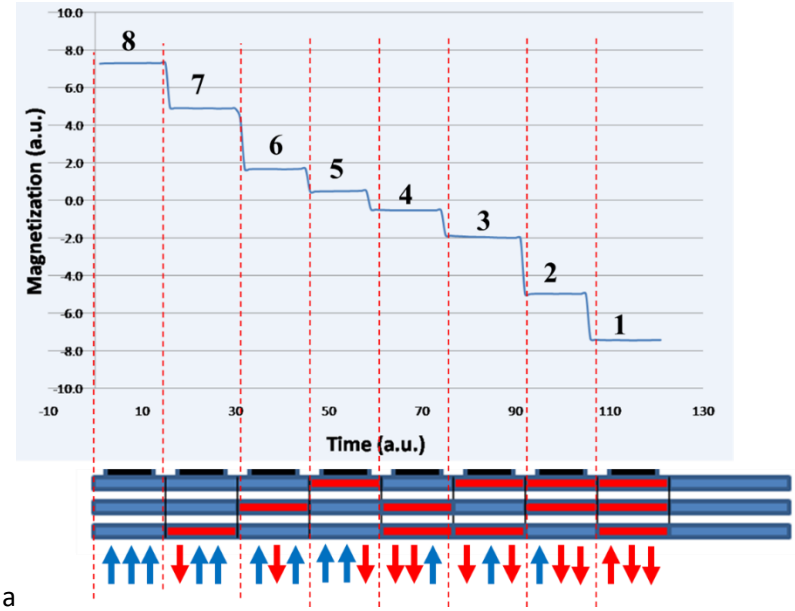

a

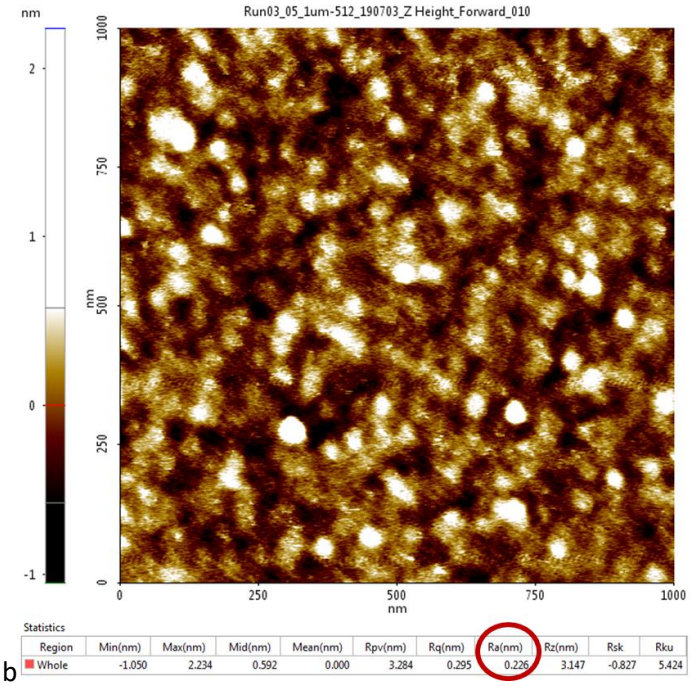

b

Figure 6: (a) F-MOKE signals measured from a 3-layer 3-D media with a net thickness of less than 20 nm. The spin configuration in the three layers corresponding to the 8 possible configurations are shown in the bottom row under the respective measured signals. (b) AFM image of the surface of a typical multilayer-based 3-D media.

Year 2 Progress Report (2019-2020)

Air Force Office of Scientific Research (AFOSR)
Title: "Energy-efficient Sub-5-nm Magnetic Tunneling Junctions"
AFOSR award #: FA9550-18-1-0527
AFOSR Program Officer: Ali Sayir
PI: Osama Mohammed (original PI: Sakhrat Khizroev), Florida International University
Date: July 21, 2020

Summary

Researchers:
Several student and postdoctoral researchers have been employed at Florida International University (FIU) to work on this project. They include:
(1). Torres, Ingrid: Ph.D. Graduate Student (Hispanic American, Female, scheduled to graduate this year)
(2). Navarrete, Brayan: Ph.D. Graduate Student (Hispanic American, scheduled to graduate this year)
(3). Toledo, Dennis, Graduate Student (Hispanic American)
(4). Wang, Ping: Ph.D. Graduate Student (graduated Summer 2020)
(5). Dean, Nathaniel: Undergraduate Student (moved to the PhD graduate school at UC-Irvine)
(6). Smith, Isadora Takako: Undergraduate Student (Female) (won a NSF REU scholarship in 2020)
(7). Stimphil, Emmanuel: Post-doctoral Researcher (African American)
(8). Nagesetti, Abhignyan: Post-doctoral Researcher

Main Accomplishments:

- Finalized 3- and 4-layer multilevel 3D device design and prototype construction. For the first time demonstrated 3- and 4-layer devices with uniform properties over an entire wafer with a characteristic size in the millimeter range. These measurements were conducted via alternating gradient magnetometry (AGM). For comparison, in the past, such structures have been shown to work only locally using focused magneto-optical Kerr effect (f-MOKE) measurements. Currently, we are working on the preparation of a peer-review paper to discuss the novel fabrication and measurement techniques for such high-uniformity 3D multilevel nanodevices.
- We have further advanced in fulfilling the goal to conduct magnetotransport measurements of multilevel 3D devices (suitable for extremely high data densities and extremely low energy consumption). To remind, these nanodevices use (i) a 3rd spatial dimension to densely pack information and (ii) exploit multilevel signal processing (versus binary processing in traditional devices). We have shown that Co/Pd and Co/Pt based nanomagnetic multilayers can provide multivel signal using giant magnetoresistance (GMR) to read back information and spin-transfer torque (STT) to write information in 3D nanodevices. In addition, this year, in collaboration with the research teams of Dr. Jeongmin Hong and Dr. Jeffrey Bokor, we have expanded this effort to build 3D nanomagnetic devices which could imitate computing operations in the brain [1]. Indeed, the neural network of the brain does not follow a simple binary logic, it is definitely multilevel. Therefore, we have started collaboration to build first truly neuromorphic computers

based on our 3D multilevel nanodevices. To maximize the number of accessible signal levels, we have introduced the so called "dual-barrier-and-domain magnetic tunneling junction (dd-MTJ) (DD) in which each layer of the 3D multi-level cell is made of two magnetic domains and thus effectively equivalent of two bits (instead of one). Thus, a n-layer dd-MTJ cell would have $2 \times 2^n = 2^{n+1}$ signal levels. We have successfully built first prototypes on the novel device concept. Details of this work have been described in the paper we recently submitted for publication in *Advanced Intelligent Systems* [3].

- Finalized the design and fabrication of coreshell magnetoelectric nanostructures (MENPs) with a size controlling ranging from below 5 to over 50 nm. Using a single-nanoparticle level nanoprobe technique, we have demonstrated record high magnetoelectric (ME) values (on the order of 10 V/cm/Oe) in these 0-3 two-phase systems. It is a truly significant achievement because such value nanostructures can unlock many novel applications ranging from nanoelectronics to nanomedicine. We just have our peer-review paper on this work published in the high-impact journal of Nano Letters [3]. In addition, the physics of the transition between the magnetostrictive core and the piezoelectric shell of such structures are described in the paper we recently submitted for publication in the Journal of Magnetism and Magnetic Materials (JMMM) [4].

Outreach Accomplishments:

- Three Graduate Students (Three Hispanic American Student Including One Woman) from underrepresented groups have been involved in this effort (see above).
- Two Female Students (One Graduate Student and One Undergraduate Student) have been involved in this research (see above).
- Two Undergraduate Students (Including One Woman) have been involved (see above).
- This year, we have established collaboration with Dr. Jeongmin Hong and Dr. Jeffrey Bokor to extend our multilevel 3D technology to the emerging field of neuromorphic computing. (Just submitted a joint paper to *Advanced Intelligent Systems* [2])

Goals for Year 3:

- Bring to completion magnetotransport measurements of magnetoelectric nanodevice, preferably conduct cryogenic measurements to confirm the novel physics under study.
- Complete design and fabrication of a 3D nanodevice based on the spin-transfer torque (STT) effect to record into the described 3-D magnetic nanostructures. (Alternatively, build a device based on the giant magnetoresistance (GMR) or tunneling magnetoresistance (TMR) to read information back from the described 3-D magnetic nanostructures.) Particularly, continue research on dd-MTJs which allow further doubling of signal levels in 3D nanodevices and explore transition into the emerging field of neuromorphic computing.

Peer-reviewed Publications where the current AFOSR grant was acknowledged:

1. P. Wang, E. Zhang, D. Toledo, I.T. Smith, B. Navarrete, N. Furman, A.F. Hernandez, M. Telusma, D. McDaniel, P. Liang, and S. Khizroev, "Colossal magnetoelectric effect in coreshell magnetoelectric nanoparticles," *Nano Letters*, doi.org/10.1021/acs.nanolett.0c01588, 2020

2. S. Khizroev and P. Liang, “Engineering future medicines with magnetoelectric nanoparticles: wirelessly controlled, targeted therapies,” *IEEE Nanotechnology Magazine* **14** (1): 23-29; 10.1109/MNANO.2019.2952227
3. P. Wang, D. Toledo, E. Zhang, M. Telusma, D. McDaniel, P. Liang, S. Khizroev, “Scanning probe microcopy study of cobalt ferrite-barrium titanate coreshell magnetoelectric nanoparticles,” accepted with minor revisions to Journal of Magnetism and Magnetic Materials (JMMM), 2020
4. J. Hong, X. Li, N. Xu, H. Chen, S. Cabrini, S. Khizroev, J. Bokor, L. You, “A dual magnetic tunnel junction based neuromorphic device,” submitted to *Advanced Intelligent Systems*, June 28, 2020
5. M. Pardo, E. Roberts, K. Pimentel, Y. Akin, B. Navarrete, P. Wang, E. Zhang, P. Liang, and S. Khizroev, “Size-dependent intranasal administration of magnetoelectric nanoparticles for targeted brain localization,” submitted to *Nanomedicine: NBM*, July 23, 2020.

Peer-reviewed Conference Presentations

J. Hong, O. Lee, S. Khizroev, J. Bokor, L. You, “Spin transfer torque (STT) magnetic recording,” accepted for presentation at the most selective annual meeting in the magnetic recording industry, The 31 Magnetic Recording Conference (TMRC) 2020, Berkeley, CA 2020, August 17-20, 2020.

Detailed Description of Research Activities

(1). Building High-Uniformity 3- and 4-layer 3D Nanodevices Using The Innovative Approach of “Artificial” Magnetic Layers

Summary: We have finalized 3- and 4-layer multilevel 3D device design and prototype construction. For the first time demonstrated 3- and 4-layer devices with uniform properties over an entire wafer with a characteristic size in the millimeter range. These measurements were conducted via alternating gradient magnetometry (AGM). For comparison, in the past, such structures have been shown to work only locally using focused magneto-optical Kerr effect (f-MOKE) measurements. Currently, we are working on the preparation of a peer-review paper to discuss the novel fabrication and measurement techniques for such high-uniformity 3D multilevel nanodevices.

The major element of this device is the multilayer magnetic structure capable of storing and controlling multilevel information recorded across in the different layers across the entire thickness of the 3D stack. Co-sputtering was the major method selected due to the advantage it offers of better thickness control at nanometer values and adequate uniformity over the entire wafer. The multilayered magnetic structure is mainly composed of Cobalt (Co), Palladium (Pd), and Titanium (Ti). To achieve adequate uniformity, it is important to optimize deposition of each layer in the stack. Film characterization consists of depositing a thin film of the metal, for a set duration of time under specific conditions. Once the film is deposited, then the thickness is measured, then the deposition rate calculated. With the deposition rate known, the timing to grow a metallic film of thickness in the nanometer scale cane be estimated. It is known that when cobalt is layered with palladium, creating Co/Pd bilayers, together they show perpendicular magnetic anisotropy and when several are stacked together, this interface induced perpendicular anisotropy further increases until a certain saturation thickness. Our challenge was due to the fact that our sputtering system didn’t have the ability to have several source guns on during the deposition. Therefore, after each material deposition step, the gun of the corresponding material should go through some preconditioning to compensate for some delay affects. This allowed the possibility to create smooth

and continuous “Artificial Magnetic Layers” composed of several Co/Pd layered stacks. To remind, our earlier 3D structures were characterized with f-MOKE technique which was provided a highly limited localization area (on the order of microns) and thus the first structures could not be optimized at the adequate waver size scale. In contrast, now the magnetic characterization has been performed using the Lakeshore alternating gradient magnetometer (AGM), as described below, as shown in Fig. 1.

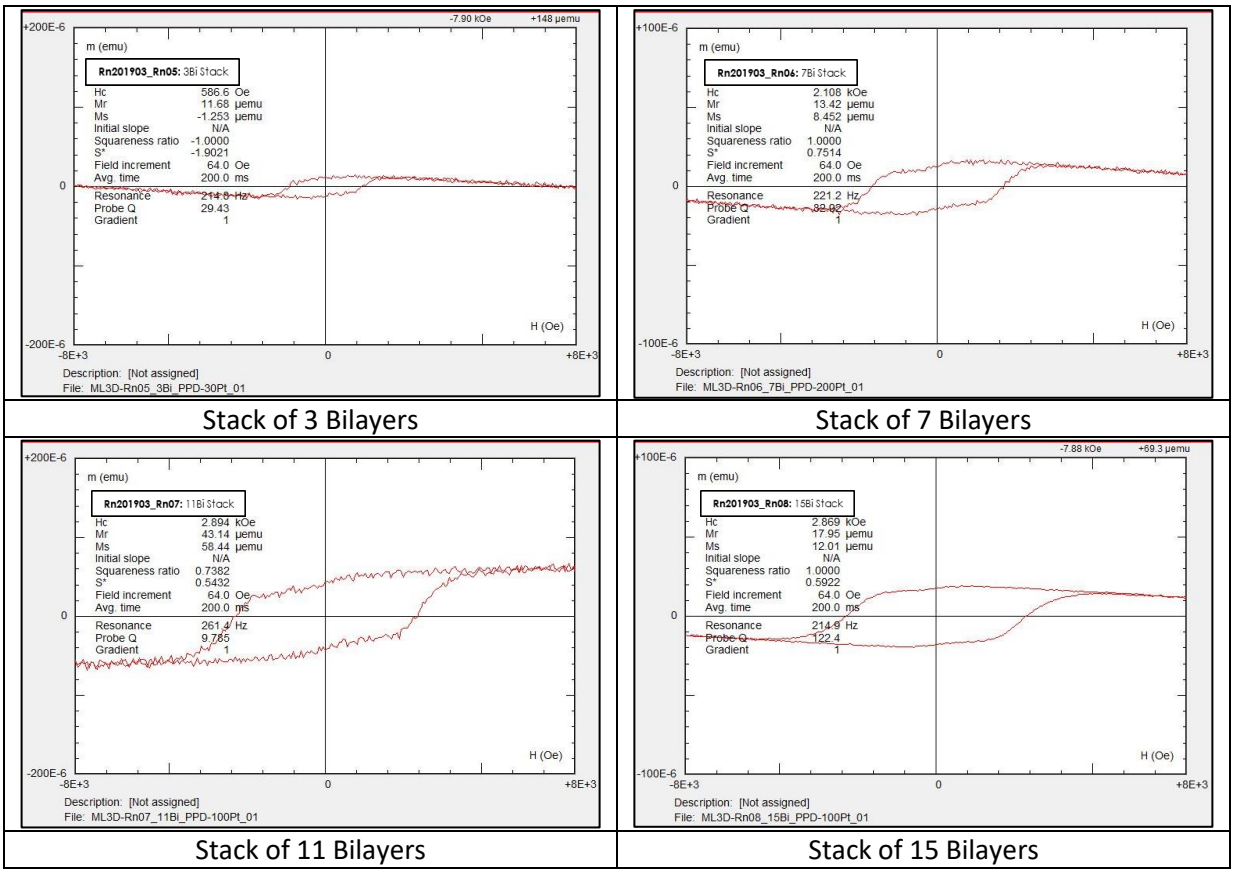

Figure 1: M-H loops (taken by AGM) of “artificial magnetic layers” of different thicknesses defined by the number of bilayers (3, 7, 11, and 15).

Once configuration for one “Artificial Magnetic Layer” is obtained, with its coercivity controlled through the number of layers in the stack, the Multilevel 3D magnetic structures are built. Here, Titanium plays a significant role as it magnetically decouples artificial magnetic layers that are on top of each other, allowing these layers to be addressed separately. Many samples have been prepared to be characterized using state-of-the-art scanning probe microscopy (SPM) characterization techniques, such as AFM/MFM/STM, f-MOKE, and VSM, some unavailable at Florida International University, but available at our partner institutions UC Berkeley (Marvell NanoLab), to study the texture and signals coming from the multilayered nanomagnetic structures. The analysis obtained at UC Berkeley helped detect that when there was more than one Artificial Magnetic Layers, not all were completely decoupled magnetically. Additionally, some samples did not present any signal on the f-MOKE instrument because its coercivity was much higher than the capacity of the machine, in those instances high field vibrating sample magnetometry (VSM) analysis has been performed, as shown in Fig. 2.

Sample	AFM	MFM	VSM

Run06 _ 1L Stack: 11Bi	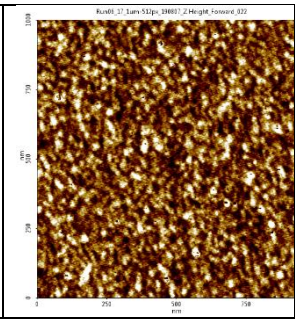	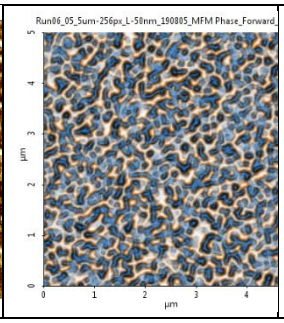	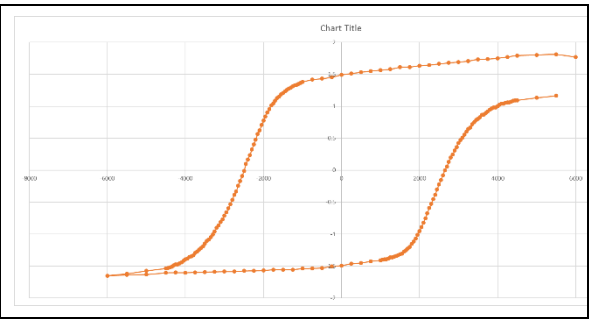

Figure 2: Atomic and magnetic force microscopy (AFM and MFM) images of "artificial magnetic layers" with a relatively very high anisotropy (~1T). (right) M-H loops (taken by VSM) of the artificial layer.

After several analysis iterations with different stacks of varying Co/Pd bilayers, it was observed through AFM characterization that as the stacks grow in the number of layers, the roughness of the sample increases as well, not suprisingly. Additionally, images of the magnetic domains of the samples have been obtained through MFM analysis. Here the stack with 11 bilayers displaying well defined domains in the shape of contrasting spots, which is characteristic of perpendicular magnetic anisotropy. Using VSM, it has been evident that the stack of 11 bilayers had the highest coercivity values (on the order of 1 T) of the samples under study. Fig. 3 the AFM/MFM images and the M-H loop (taken by f-MOKE) of the sample that yielded the most promising two magnetically decoupled artificial magnetic layers.

Sample	**AFM**	**MFM**	**MOKE - Perpendicular**
Run03_ 2L Stack: 3Bi/11Bi	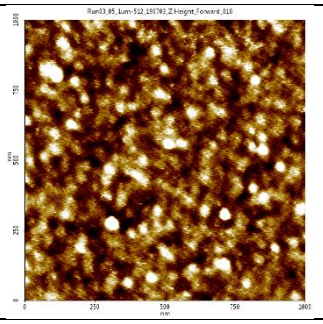	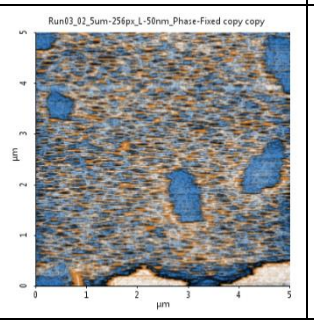	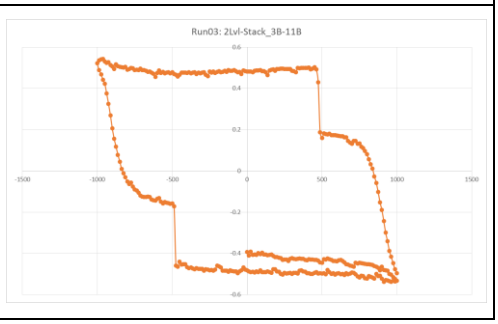

Figure 3: AFM/MFM images and (right) M-H loop (taken by f-MOKE) of the sample that yielded the most promising two magnetically decoupled artificial magnetic layers.

Consequently, the processes and recipes have been reviewed and improved, so that modifications have been made on the machine's hardware to successfully magnetically decouple more combinations of two different stacks. Several combinations have been made and after the two magnetic layers have obtained, then a 3-D multilevel magnetic media with three and four magnetic layers have been constructed, as shown in Fig. 4.

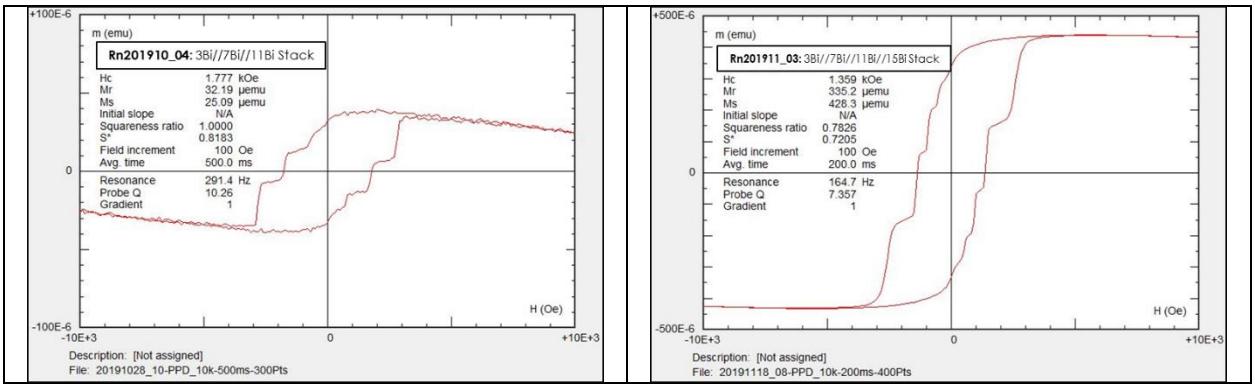

Figure 4: M-H loops of 3- and 4-layer artificial 3D magnetic media taken by AGM.

(2). Magnetotransport Measurements Through High-Uniformity 3- and 4-layer "Artificial 3D Nanodevices"

Summary: We have further advanced in fulfilling the goal to conduct magnetotransport measurements of multilevel 3D devices (suitable for extremely high data densities and extremely low energy consumption). To remind, these nanodevices use (i) a 3rd spatial dimension to densely pack information and (ii) exploit multilevel signal processing (versus binary processing in traditional devices). We have shown that Co/Pd and Co/Pt based nanomagnetic multilayers can provide multivel signal using giant magnetoresistance (GMR) to read back information and spin-transfer torque (STT) to write information in 3D nanodevices. In addition, this year, in collaboration with the research teams of Dr. Jeongmin Hong and Dr. Jeffrey Bokor, we have expanded this effort to build 3D nanomagnetic devices which could imitate computing operations in the brain [1]. Indeed, the neural network of the brain does not follow a simple binary logic, it is definitely multilevel. Therefore, we have started collaboration to build first truly neuromorphic computers based on our 3D multilevel nanodevices. To maximize the number of accessible signal levels, we have introduced the so called "dual-barrier-and-domain magnetic tunneling junction (dd-MTJ) (DD) in which each layer of the 3D multi-level cell is made of two magnetic domains and thus effectively equivalent of two bits (instead of one). Thus, a n-layer dd-MTJ cell would have 2 x 2^n = 2^{n+1} signal levels. We have successfully built first prototypes on the novel device concept. Details of this work have been described in the paper we recently submitted for publication in *Advanced Intelligent Systems* [3].

The mechanism of recording via the STT effect into thus fabricated artificial 3-layer 3D nanostructure is illustrated in Fig. 5. In this case, there are 2^3=8 magnetic states, which can be distinguished from each other either optically, e.g., through f-MOKE measurements, or magnetically, e.g., through partial M-H loops. If using the above GMR effect, only three distinct levels can be distinguished because there are only three fundamentally different magnetic interfaces between the three magnetic layers, as illustrated in Fig. 5 (left bottom). Thus, the resistance between any two adjacent layers can have only three different values. A measured I-V curve corresponding to the three resistance states is shown in Fig. 5 (right top). The control sequence (sequential application of currents) to switch between these three states is shown in Fig. 5 (right bottom).

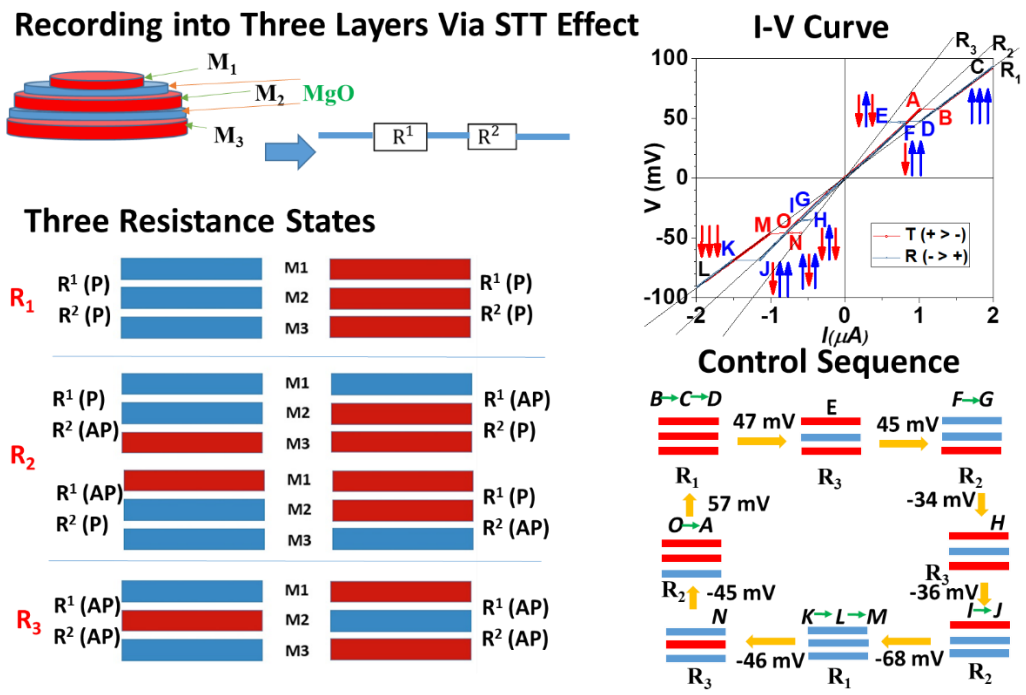

Figure 5: Illustration of the mechanism of STT recording into thus fabricated artificial 3-layer 3D nanostructure. (Left right) Three distinct GMR states in the 3D stack. (right top) An experimental I-V curve corresponding to the three resistance (GMR) states. (Right bottom) The control sequence (sequential application of currents) to switch between these three states.

As for the novel dd-MTJ concept which allows 2^{n+1} signal levels from each n-layer cell, we have completed our first prototypes. The protypes were built based on the results of comprehensive micromagnetic simulations. The dd-MTJ device uses a spin-polarized current, according to the STT effect, to generate 8 resistive signal levels from a 3-layer 3D artificial nanostructure. The doubling of the signal levels is due to the resistive switching in the spin-torque memristor due to the displacement of a magnetic domain wall by spin-torques in a perpendicularly magnetized magnetic tunnel junction. The concept is consisely illustrated in Fig. 6.

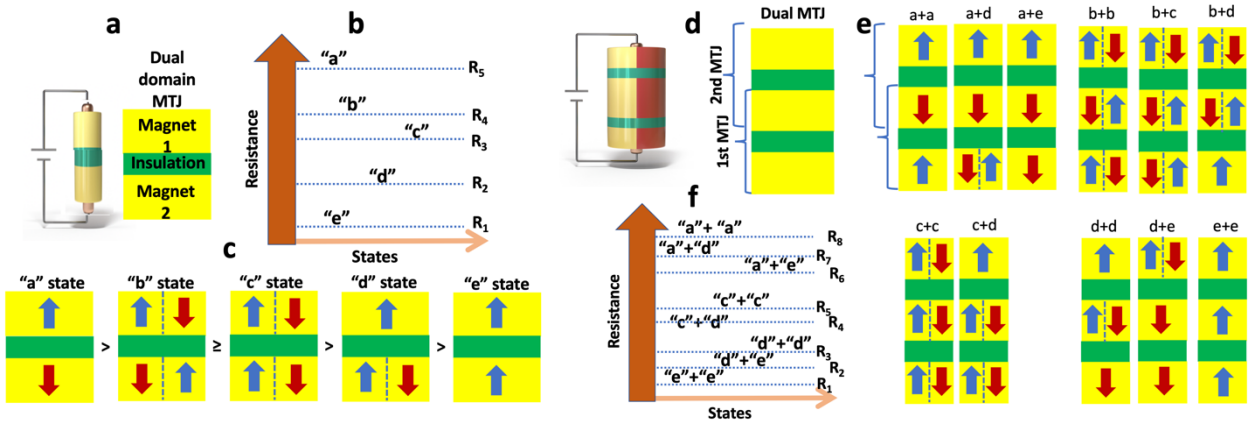

Figure 6: Schematics of the model of dual domain MTJs (dMTJs) and dual barrier/dual domain MTJs (ddMTJs) and their resistance values in each ideal configuration. **(a)** Dual Domain MTJs (ddMTJs) are

shown in the left /right parts, respectively. The structures consist of two magnets with an insulation. And **(b)** the corresponding resistance values of each ideal state could be 5 different resistance values. **(c)** The different resistance states could have the following configurations of the resistance. Among all of the 5 arrangements in the dual domain MTJ, there are 2 resistance states (except for states "b", "c", "d") in each junction structure. From the nature of domain orientation, "b" "c" "d" states are usually ignored for the inherent domain orientation due to the Oersted field. The yellow boxes represent magnets and the red and blue arrows show magnetization directions: either up or down. Two arrows in a yellow box denote dual domain magnetization. **(d)** Possible scenario of switching in ddMTJs. As the current continues to be applied, magnetization in M_1, M_2 and M_3 may change with the arrow direction. **(e)** Depending on the orientation of each magnet, 8 distinguishable resistance values could be observed. Among all of the 5 arrangements in the dual domain MTJ, there are 4 resistance states (except for state "b") in each junction structure. From the nature of domain orientation, "b" state is ignored for the inherent domain orientation due to the Oersted field. **(f)** Resistance values of the following states could be possible from 1 to 8. The corresponding configurations of the resistance states are shown next to the resistance values.

Based on preliminary micromagnetic simulation using the NIST open source simulator OOMMF, we have built our ddMTJ devices. Their magnetic properties are summarized in Fig. 7. The focused ion beam (FIB) fabricated device is shown in Fig. 7a. A high-resolution Helium Ion-beam Microscope (HIM) was used to obtain the high resolution image. The 3D device is made of three artificial (synthetic) ferromagnets (FMs), deposited through co-sputtering, with thickness values of 0.9, 1.3, and 1.6 nm, respectively. Their diameters were approximately 100, 110, and 120 nm, respectively. The right insert of Fig. 7a shows a high-resolution transmission electron microscopy (TEM) image of the cross-section of the 3D stack. Accordingly, two MTJs were stacked in series to form the ddMTJ structure. The MFM image shown in the insert of Fig. 7a confirms the dual domain structure in each FM. Bright and dark colors show two domains in the structure. A M-H loop of the structure (taken with f-MOKE) is shown in Fig. 7b. By applying a magnetic field, the three FMs in the stack show distinctive magnetic properties displaying different values of the coercive field and the saturation magnetization. The eight possible distinct values of the resistance of such ddMTJ devices are illustrated in Fig. 7c. According to the earlier done micromagnetic simulations, a current pulse is needed to switch between the resistance states, while the current density and the pulse duration are non-unique when the current is larger than the critical current density. It is noteworthy that some states, which are shown with two digits, e.g., 7-1, are unstable, therefore, we don't study them in this case. The numbers are based on the resistance values from lowest to highest. The details of this study are described in the paper we just submitted to *Advanced Intelligent Systems* [2].

In the near future, we will continue fabrication and characterization of these novel artificial (synthetic) multilevel 3D nanodevices.

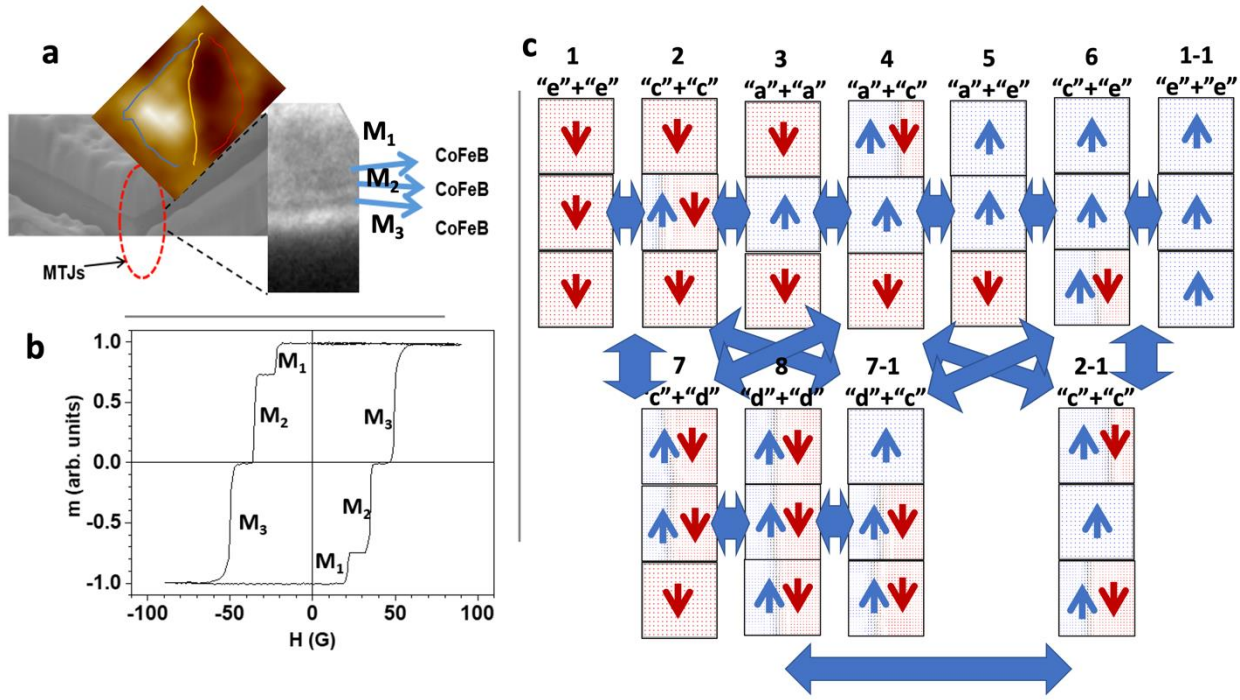

Figure 7. Magnetic properties of the first built ddMTJ prototype. **(a)** Ultra-high resolution of He-ion beam image (left) and TEM image (right) of the device stacks. An MFM image of dual domain structures. Here, indication line shows there is only one domain wall, that is a dual magnetic domain, at demagnetization state in the device. **(b)** m-H loop of the device stacks. **(c)** OOMMF simulation of how the signal in a dual MTJ propagates. Red arrows show that the resistance values can be determined according to the following orders: the domain structures/states are numbered according to the order of the appearance: eight different resistance states "e+e", "c+c", "a+a", "a+c", "a+e", "c+e", "c+d", "d+d" are named as R_1, R_2, R_3, R_4, R_5, R_6, R_7, and R_8, respectively for the corresponding domain structures. The numbers are based on the resistance values from the lowest to highest. Beyond that, different domain structures may correspond to onesame resistance value, for example, "2" and "2-1" have the same resistance value of "c+c." According to the simulation results, we found that the state "d+d" is unstable between state 7 and 7–1, for the given values of the anisotropy energies, as described below.

(3). Characterization of new types of MENPs

Summary: We have finalized the design and fabrication of coreshell magnetoelectric nanostructures (MENPs) with a size controlling ranging from below 5 to over 50 nm. Using a single-nanoparticle level nanoprobe technique, we have demonstrated record high magnetoelectric (ME) values (on the order of 10 V/cm/Oe) in these 0-3 two-phase systems. It is a truly significant achievement because such value nanostructures can unlock many novel applications ranging from nanoelectronics to nanomedicine. We just have our peer-review paper on this work published in the high-impact journal of Nano Letters [3]. In addition, the physics of the transition between the magnetostrictive core and the piezoelectric shell of such structures are described in the paper we recently submitted for publication in the Journal of Magnetism and Magnetic Materials (JMMM) [4].

References:

[1] S. Khizroev and P. Liang, “Engineering future medicines with magnetoelectric nanoparticles: 10.1109/MNANO.2019.2952227

[2] J. Hong, X. Li, N. Xu, H. Chen, S. Cabrini, S. Khizroev, J. Bokor, L. You, “A dual magnetic tunnel junction based neuromorphic device,” submitted to *Advanced Intelligent Systems*, June 28, 2020

[3] P. Wang, E. Zhang, D. Toledo, I.T. Smith, B. Navarrete, N. Furman, A.F. Hernandez, M. Telusma, D. McDaniel, P. Liang, and S. Khizroev, “Colossal magnetoelectric effect in coreshell magnetoelectric nanoparticles,” *Nano Letters*, doi.org/10.1021/acs.nanolett.0c01588, 2020

[4] P. Wang, D. Toledo, E. Zhang, M. Telusma, D. McDaniel, P. Liang, S. Khizroev, “Scanning probe microcopy study of cobalt ferrite-barrium titanate coreshell magnetoelectric nanoparticles,” accepted with minor revisions to Journal of Magnetism and Magnetic Materials (JMMM), 2020

Year 3 Progress Report (2020-2021)

Air Force Office of Scientific Research (AFOSR)
Title: "Energy-efficient Sub-5-nm Magnetic Tunneling Junctions"
AFOSR award #: FA9550-18-1-0527
AFOSR Program Officer: Jiwei Lu
PI: Osama Mohammed (original PI: Sakhrat Khizroev), Florida International University
Date: November 11, 2021

Summary

Researchers:
Several student and postdoctoral researchers have been employed at Florida International University (FIU) to work on this project. They include:
(1). Torres, Ingrid: Ph.D. Graduate Student (Hispanic American, Female, graduated Fall 2021)
(2). Navarrete, Brayan: Ph.D. Graduate Student (Hispanic American, graduated Spring 2021)
(3). Toledo, Dennis, Graduate Student (Hispanic American)
(4). Smith, Isadora Takako: Undergraduate Student (Female) (won a NSF REU scholarship in 2020)
(5). Campos Alberteris, Manuel: Post-doctoral Researcher (Hispanic American)

Main Accomplishments:

- Completion of a 8-level STT-based neuromorphic device synthesis and characterization.
- Using Magnetoelectric Nanoparticles (MENPs) As 3D Building Blocks in Next-generation Nanoscale Devices

Outreach Accomplishments:

- Three Graduate Students (Three Hispanic American Student Including One Woman) from underrepresented groups have been involved in this effort (see above).
- Two Female Students (One Graduate Student and One Undergraduate Student) have been involved in this research (see above).
- Two Undergraduate Students (Including One Woman) have been involved (see above).
- This year, we have established collaboration with Dr. Jeongmin Hong and Dr. Jeffrey Bokor to extend our multilevel 3D technology to the emerging field of neuromorphic computing. (Just submitted a joint paper to *Advanced Intelligent Systems* [2])

Peer-reviewed Publications where the current AFOSR grant was acknowledged:

[1]. J. Hong, X. Li, N. Xu, H. Chen, S. Cabrini, S. Khizroev, J. Bokor, L. You, "A dual magnetic tunnel junction-based neuromorphic device," *Advanced Intelligent Systems*: 2000143 (2020)

[2]. R. Guduru, P. Liang, A. Hadjikhani, P. Wang, V. Musaramthota, A. Franco Hernandez, B. Arkook, J. Hong, S. Khizroev, "Magnetically controlled crystallographic properties of graphite sheets with self-assembled periodic arrays of magnetoelectric nanoparticles," *Appl. Surf. Science* **573**: 151455 (2021).

[3]. P. Wang, D. Toledo, E. Zhang, M. Telusma, D. McDaniel, P. Liang, **S. Khizroev**, "Scanning probe microcopy study of cobalt ferrite-barium titanate coreshell magnetoelectric nanoparticles," JMMM 516: 167329 (2020).

[4]. T. Nguyen, J. Gao, P. Wang, A. Nagesetti, P. Andrews, S. Masood, Z. Vriesman, P. Liang, S. Khizroev, X. Jin, "In vivo wireless brain stimulation via non-invasive and targeted delivery of magnetoelectric nanoparticles," *Neurotherapeutics* **18** (3): 2091-2106 (2021); doi: 10.1007/s13311-021-01071-0.

[5]. M. Pardo, E. Roberts, K. Pimentel, Y. Yildirim, B. Navarrete, P. Wang, E. Zhang, P. Liang, **S. Khizroev**, "Size-dependent intranasal administration of magnetoelectric nanoparticles for targeted brain localization," *Nanomedicine: NBM* **32**: 102337 (2021).

Detailed Description of Research Activities in Year 3

(1). Building 3- and 4-layer "Artificial 3D Nanodevices" Suitable For Implementation of Neuromorphic Computing

In Year 2, we advanced in fulfilling the goal to conduct magnetotransport measurements of multilevel 3D devices (suitable for extremely high data densities and extremely low energy consumption). To remind, these nanodevices use (i) a 3rd spatial dimension to densely pack information and (ii) exploit multilevel signal processing (versus binary processing in traditional devices). We showed that Co/Pd and Co/Pt based nanomagnetic multilayers could provide multivel signal using giant magnetoresistance (GMR) to read back information and spin-transfer torque (STT) to write information in 3D nanodevices. Furthermore, we built a strong research collaboration with Jeongming Hong and Jeffrey Bokor (UC-Berkeley) with who whom we worked to translate our multilevel 3D device technology to built first neuromorphic computer devices (to imitate computing operations in the brain).

In Year 3, the results of our collaboration to implement our multilevel 3D technology in the neuromorphic computing application were presented in detail in a peer-review publication [1]. To remind, in this configuration, we not only physically divided each 3D element into layers but also introduced a domain wall in each layer, thus introducing two domains in each layer. Consequently, we referred to such a 3D element as a "dual-barrier-and-domain magnetic tunneling junction (dd-MTJ) (DD)" element. In other words, each layer of the element contains 2 bits instead of the traditional one bit of information. Thus, a n-layer dd-MTJ cell would have $2 \times 2^n = 2^{n+1}$ signal levels. As described in detail in this peer-reviewed paper, based on micromagnetic simulations and using a multi-ion focused ion beam (MI-FIB) we have successfully built first prototypes of the novel device concept. In this device, we used a spin-polarized current, according to the STT effect, to generate 8 resistive signal levels from a 3-layer 3D artificial nanostructure. Hence, the doubling of the signal levels is due to the resistive switching in the spin-torque memristor due to the displacement of a magnetic domain wall by spin-torques in a perpendicularly magnetized magnetic tunnel junction.

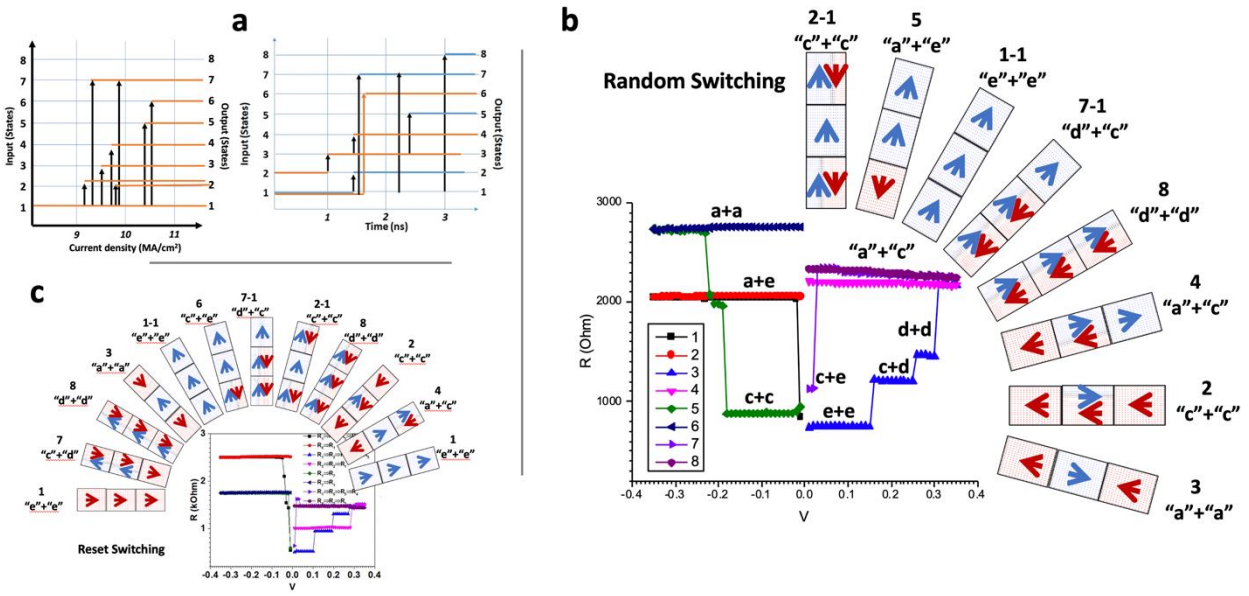

Figure 1. A scenario of the 8-level signal processing using spin computers and resulting simulation data. *resistance modulation by train of identical narrow pulses with fixed amplitude, potentiation and depression* **(a)** With the change of applied current pulse, the magnetization was switched in the direction of the arrows which are consistent with the envisaged switching scenario and the resulting inputs and outputs. **(b)** Programmable neurocomputing device and 8-level signal processing. Inset represents the signal switched from 1 to other states by varying switching energy. Random switching after demagnetization. **(c)** Reset switching after magnetization. Resistance measurements data of reset switching.

For neurormorphic computing (hardware implementation of artificial neural network (ANN)) there are a number of metrics that have to be reached, in order for the proposed technology to be viable. One of those is the ability to tune the synaptic weight, which can be represented by a conductance/resistance in a controlled but "blind" manner**.** *The ideal case of the device could be switched in a linear and symmetric fashion which is critical for efficient neuromorphic computing.*

The proposed ddMTJ element could be switched between the eight possible resistive states by application of the voltage sequence, as illustrated in Fig. 1a. Using the public-domain simulation package OOMMF by NIST, we simulated the current density of the applied current and the corresponding pulse duration required to switch the magnetization states. The proper values of stimulation were determined from the spike timing dependence plasticity (STDP) measurements. Typical magnetization configurations leading to 8 signals are shown in Fig. 2b. By sweeping the voltage according to the simulated patterns (Fig. 2b), the outputs could be gradually changed from the lowest to highest value. The eight distinct resistance values were observed for the shown voltage programming, from -0.35 to 0.35 V within the range of the switching energy.
Considering the resistance and voltage programming values, the switching energy ranged from 4 to 10 MA/cm^2. It can be noted that R_4 and R_5 were unstable because of the relatively anisotropy energy in the states, as described in the paper. The experimental data were compared with the simulation results. Current density dependence from IV measurements is shown in Figs 1b and c. In the case of the current applied from top to bottom in the stack, evolution of the states could be

carried on uni–directionally following the arrow direction as shown in Fig. 1b. Thus, each state could be switched to the state behind it with a current pulse applied in the case of random switching. The magnetization in the reset state is shown in Fig. 4c. Multiply-Accumulate action could be physically performed through resonance current pulses. Each state could be defined through the switching energy and time. We also showed that the current pulses with different switching energy could be performed to have vector-matrix multiplication. Last but not least, the described operation of the novel MTJs device clearly indicated the 3D junction could be also used as one-byte operation spin computers. In addition, the results enabled a new computer paradigm for ultra-low power future spin based neuromorphic computing.

(2). Using Magnetoelectric Nanoparticles (MENPs) As 3D Building Blocks in Next-generation Nanoscale Devices

Last year, we learned how to fabricated core-shell MENPs with record high magnetoelectric (ME) coefficient. Earlier, we also showed how nanoparticles could be used for spintronics-based energy-efficient computation. This time, we showed that MENPs could be used as 3D building blocks in next generation devices by integrating them into graphite multilayered structures. This year, we published the main results of this effort in a peer-reviewed paper [2]. Particularly, in this study, 30-nm CoFe2O4–BaTiO3 core–shell MENPs were embedded into graphite sheets to enable external control of intrinsic properties such as the intercalation process. The embedded nanoparticles were self-assembled into a honeycomb pattern with a characteristic period on the order of 200 nm, as confirmed through energy-dispersive spectroscopy (EDS) by scanning electron microscopy (SEM) as well as through atomic and magnetic force microscopy (AFM and MFM) (Fig. 2). Integration of the nanoparticles into the graphite structure was also confirmed through Fourier transform infrared (FT-IR) imaging and X-Ray diffraction (XRD) analysis. XRD measurements indicated crystallographic changes in the response to application of a 500-Oe magnetic field. M-H measurements by vibrating sample magnetometer (VSM) showed the coercivity of the nanoparticles dropped from approximately 300 Oe to below 200 Oe when the nanoparticles were embedded into the aforementioned self-assembled patterns into the graphite matrix. The measurements clearly indicated that MENPs could be used as both computing and building blocks in future 3D nanoelectronics devices.

A

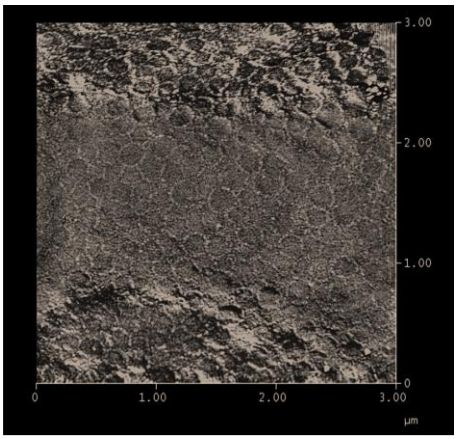

B

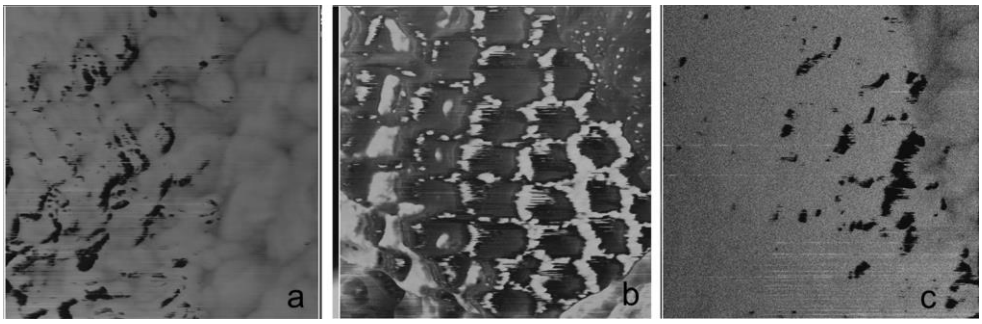

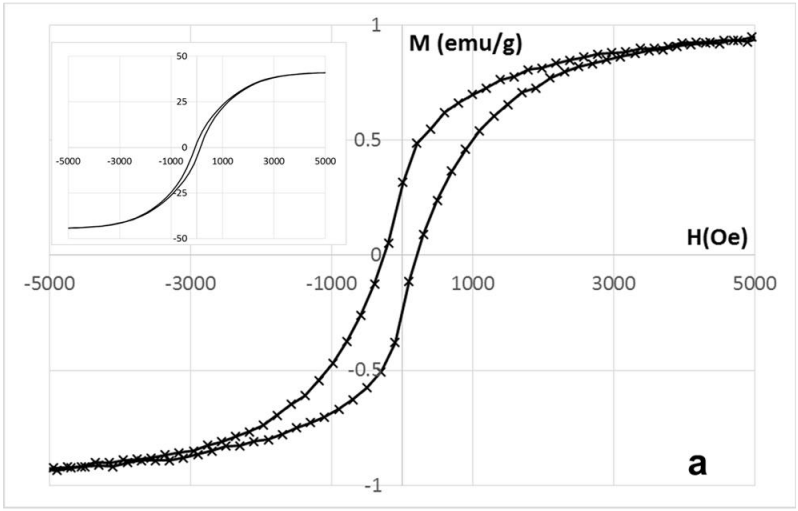

C

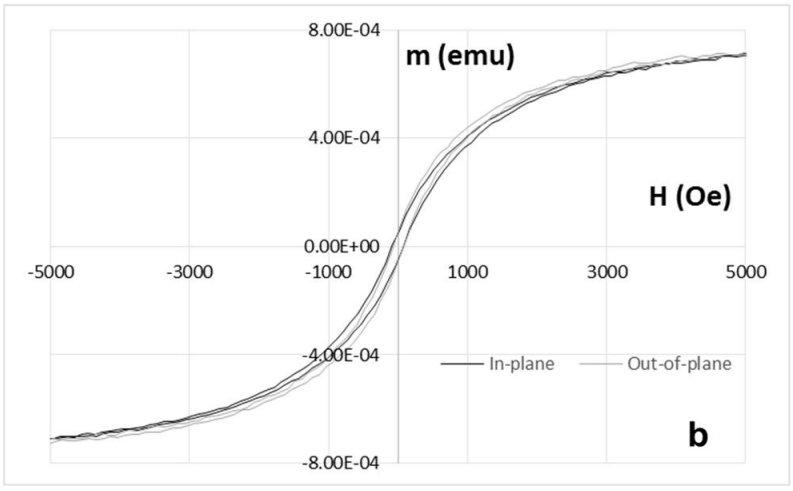

Figure 2: (**A**). AFM image of the top surface of a graphite anode with MENPs embedded at a concentration of 17% to the weight of the anode. A honeycomb pattern of the self-assembled nanoparticles can be seen. (**B**). MFM images of a zoomed-in region on the top surface of a graphite anode with embedded MENPs at different magnetic fields: (a) 0 Oe, (b) 500 Oe, (c) - 500 Oe. The characteristic size of each hexagon is on the order of 200 nm. (**C**): (a) M-H hysteresis loops for naked MENPs. The insert shows a loop for naked ferromagnetic (CoFe2O4) nanoparticles. (b) M-H hysteresis loop for MENPs embedded into a graphite anode with a nanoparticle concentration

of 17% with respect to the graphite weight. The embedded nanoparticles were self-assembled into a honeycomb pattern within the anode.

Based on these nanoparticles, we published 3 other peer-reviewed papers [3-5].

References:

[1]. J. Hong, X. Li, N. Xu, H. Chen, S. Cabrini, S. Khizroev, J. Bokor, L. You, "A dual magnetic tunnel junction-based neuromorphic device," *Advanced Intelligent Systems*: 2000143 (2020)

[2]. R. Guduru, P. Liang, A. Hadjikhani, P. Wang, V. Musaramthota, A. Franco Hernandez, B. Arkook, J. Hong, S. Khizroev, "Magnetically controlled crystallographic properties of graphite sheets with self-assembled periodic arrays of magnetoelectric nanoparticles," *Appl. Surf. Science* **573**: 151455 (2021).

[3]. P. Wang, D. Toledo, E. Zhang, M. Telusma, D. McDaniel, P. Liang, **S. Khizroev**, "Scanning probe microcopy study of cobalt ferrite-barium titanate coreshell magnetoelectric nanoparticles," JMMM 516: 167329 (2020).

[4]. T. Nguyen, J. Gao, P. Wang, A. Nagesetti, P. Andrews, S. Masood, Z. Vriesman, P. Liang, S. Khizroev, X. Jin, "In vivo wireless brain stimulation via non-invasive and targeted delivery of magnetoelectric nanoparticles," *Neurotherapeutics* **18** (3): 2091-2106 (2021); doi: 10.1007/s13311-021-01071-0.

[5]. M. Pardo, E. Roberts, K. Pimentel, Y. Yildirim, B. Navarrete, P. Wang, E. Zhang, P. Liang, **S. Khizroev**, "Size-dependent intranasal administration of magnetoelectric nanoparticles for targeted brain localization," *Nanomedicine: NBM* **32**: 102337 (2021).